

# Two-species percolation and Scaling theory of the metal-insulator transition in two dimensions

Yigal Meir

*Department of Physics, Ben-Gurion University, Beer Sheva 84105, ISRAEL*

Recently, a simple non-interacting-electron model, combining local quantum tunneling via quantum point contacts and global classical percolation, has been introduced in order to describe the observed “metal-insulator transition” in two dimensions [1]. Here, based upon that model, a two-species-percolation scaling theory is introduced and compared to the experimental data. The two species in this model are, on one hand, the “metallic” point contacts, whose critical energy lies below the Fermi energy, and on the other hand, the insulating quantum point contacts. It is shown that many features of the experiments, such as the exponential dependence of the resistance on temperature on the metallic side, the linear dependence of the exponent on density, the  $e^2/h$  scale of the critical resistance, the quenching of the metallic phase by a parallel magnetic field and the non-monotonic dependence of the critical density on a perpendicular magnetic field, can be naturally explained by the model. Moreover, details such as the nonmonotonic dependence of the resistance on temperature or the inflection point of the resistance vs. parallel magnetic are also a natural consequence of the theory. The calculated parallel field dependence of the critical density agrees excellently with experiments, and is used to deduce an experimental value of the confining energy in the vertical direction. It is also shown that the resistance on the “metallic” side can decrease with decreasing temperature by an arbitrary factor in the degenerate regime ( $T \lesssim E_F$ ).

PACS numbers: 71.30.+h, 73.40.Qv, 73.50.Jt

## I. BACKGROUND AND INTRODUCTION OF THE MODEL

The surprising experimental observation of a metal-insulator transition in two dimensions [2–6], in contradiction with the predictions of single-parameter scaling theory for noninteracting electrons [7], has been a subject of extensive investigation in recent years. Theories ranging from attributing the effect to scattering by impurities [8] to those suggesting “a new form of matter” [9] have been proposed. Some theories, based on the treatment of disorder and electron-electron interactions by Finkelstein [10], have been put forward [11], while other approaches considered spin-orbit scattering [12] or percolation of electron-hole liquid [13]. Altshuler et al. [8] gave several arguments why this transition is not due to a non-Fermi liquid behavior, including the fact that the exponential increase of the conductance with temperature persists to high densities where the conductance is almost two orders of magnitude larger than the critical conductance, and the fact that the Hall resistance is rather insensitive to temperature, and does not display any critical behavior. Some experimental results supporting the conclusion that the transition is not driven by interactions that were mentioned in [1] included the fact that such a transition was observed also in high-density electron gas upon the introduction of artificial disorder [14] and the fact that increasing the density in a parallel electron gas increases the conductance [6], even though the interactions are screened by the parallel gas. More recently, the compressibility on the metallic side of the transition was measured [15] and was shown to be accurately described by Hartree-Fock approximation,

again indicating a normal Fermi-liquid behavior. Several other recent experiments [16,17] have demonstrated weak-localization behavior on the metallic side with very little effect of electron-electron interactions.

Recently [1] I proposed a simple non-interacting electron model, combining local quantum tunneling and global classical percolation, to explain several features of the experimental observations. At low electron or hole densities the potential fluctuations due to the disorder cannot be screened and they define density puddles (density separation into puddles in gated GaAs was indeed observed experimentally by Eytan et al. [18], using near-field spectroscopy). These puddles are connected via saddle points, or quantum points contacts (QPCs). It is now established that even at low temperatures and for open puddles (or quantum dots), the dephasing time may be shorter than the escape time from the puddle [19]. Thus it is assumed that between tunneling events through the QPCs dephasing takes place, and the conductance of the system will be determined by adding classically these quantum resistors. (A related model was introduced by Shimshoni et al. [20] to describe successfully transport in the quantum Hall regime.) Each saddle point is characterized by its critical energy  $\epsilon_c$ , such that the transmission through it is given by  $T(\epsilon) = \Theta(\epsilon - \epsilon_c)$ . (I assume that the energy scale over which the transmission changes from zero to unity is smaller than the other relevant energy scales, to avoid additional parameters). Then the conductance through a QPC is given by the Landauer formula,

$$G(\mu, T) = \frac{2e^2}{h} \int d\epsilon \left( -\frac{\partial f_{FD}(\epsilon)}{\partial \epsilon} \right) T(\epsilon) \\ = \frac{2e^2}{h} \frac{1}{1 + \exp[(\epsilon_c - \mu)/kT]}, \quad (1)$$

where  $\mu$  is the chemical potential, and  $f_{FD}$  is the Fermi-Dirac distribution function.

The system is now composed of classical resistors, where the resistance of each one of them is given by (1), with random QPC energies.

## II. TWO-SPECIES SCALING THEORY

In [1] I presented numerical calculations to be compared to the experimental data. Here I present a different approach, based on the scaling theory of a two-species percolation network. At low temperatures the resistors can be divided into two groups, the conducting ones ( $\epsilon_c < \mu$ ), whose conductance is about  $2e^2/h$ , and the insulating ones ( $\epsilon_c > \mu$ ), whose conductance is nearly zero. Thus the distribution of the conductances will be a two-peak distribution, where the weight of each peak will be determined mainly by density (or chemical potential) and the position of the conducting peaks will be determined mainly by temperature. Since most properties of such a percolating network are insensitive to details of this distribution, I replace it by a two-delta function distribution, namely replace the network by a network comprising of two types of conductors: An effective conductor  $\sigma_m$  describing the metallic QPCs, and whose conductance is given by (1), with an appropriately averaged  $\epsilon_c$ :

$$\sigma_m = \frac{2e^2}{h} \frac{1}{1 + \exp[-A/kT]} \quad (2)$$

( $A$ , which depends on the potential fluctuations distribution, is taken as unity in the following, i.e. it defines the temperature scale), and an effective conductor  $\sigma_i$  describing the contribution of the insulating phase. The conductance of the insulating QPC is dominated by activation [21],  $\sigma_i = \sigma_a \exp[-A_1/T]$ . (Indeed, experimental investigations reported that “two different contributions to the conductivity (or two conducting systems) may exist, one with a metallic temperature behavior and another one with a standard, insulating, weak-localization behavior” [17].)

The scaling form of the two-dimensional conductance of such a two-phase mixture,  $\sigma$ , near the percolation threshold is well known [22,23],

$$\sigma = \sqrt{\sigma_m \sigma_i} f \left[ (n - n_c)^t \sqrt{\sigma_m / \sigma_i} \right] \quad (3)$$

with  $t \simeq 1.3$ , the conductance critical exponent for two-dimensional percolation, and

$$f(x) \propto \begin{cases} x & x \rightarrow \infty \\ 1/x & x \rightarrow -\infty \end{cases}, \quad (4)$$

so that in the case  $\sigma_i \rightarrow 0$  (a regular random resistor network),  $\sigma(n) \sim \sigma_m(n - n_c)^t$ , while in the case  $\sigma_m \rightarrow \infty$  (a mixture of an insulator and a superconductor),  $\sigma(n) \sim \sigma_i(n_c - n)^{-t}$ . (In the above I used the notation  $x^t \equiv \text{sign}(x)|x|^t$ .) The exact form of  $f(x)$  is not very important, and in the following I have chosen  $f(x) = \log(B + \exp[x]) / \log(B + \exp[-x])$ , with  $B = 2$ .

## III. “ZERO” TEMPERATURE

At low enough temperatures, such that  $T \ll A, A_1$  the conductors have either zero conductance or a conductance equal to  $2e^2/h$ . If the dephasing time is still finite at these temperatures, one has a random-resistor network, which exhibits a second-order percolation transition [23]. In Fig. 1 I fit the lowest-temperature experimental data of [4–6] to the expected critical dependence. Clearly, the agreement with the classical percolation prediction is excellent. Such an agreement with the classical percolation critical behavior may serve as an additional experimental indication that the dephasing is still finite at the lowest available experimental temperatures.

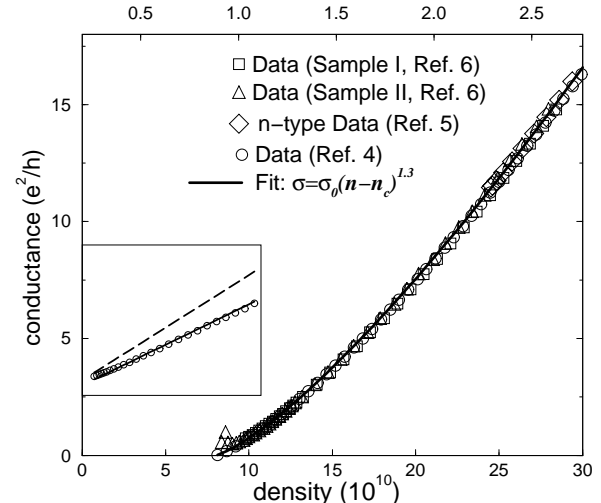


Fig. 1. Comparison of the lowest temperature data of [6] (two sets of data, triangles and squares, 330mK, density given by the lower axis) and of [4] (circles, 57mK, density given by the upper axis), and of the n-type data [5] (diamonds) to the prediction of percolation theory (solid line). Inset: Logarithmic derivative of the data [6] which gives a line whose slope is inverse of the critical exponent. The percolation prediction ( $t \simeq 1.3$ ) is given by the solid line. For comparison a  $t = 1$  slope is also shown (broken line).

In the inset I plot the experimental data [6] for  $1/(d \log \sigma / d \log n)$ , which, if indeed  $\sigma \sim (n - n_c)^t$ , is given

by  $(n-n_c)/t$ . The data indeed fits on a straight line, with a slope given by  $1/t \simeq 1/1.3$ . For comparison a straight line with a slope of unity is also depicted, in order to demonstrate that a critical exponent of unity cannot fit the data.

#### IV. TEMPERATURE DEPENDENCE OF THE RESISTANCE

As temperature increases, the Fermi-Dirac distribution is broadened. Consequently the conductance of the transparent quantum point contacts ( $\epsilon_c < \mu$ ) decreases exponentially (towards half its value), while that of the insulating ones increases. Thus we expect to see rather dramatic effects as a function of temperature. This is indeed depicted in Fig. 2. In (a) we plot the prediction of the model and in (b) the experimental data [4]. As temperature is lowered, systems with slightly different resistance at high temperatures will diverge exponentially with decreasing temperatures. The resistance of systems on the metallic side ( $n > n_c$ ) will saturate at zero temperature, while that of insulating samples will diverge, in agreement with the general shape of the experimental curves. Note that there is an upward turn even on the metallic side of the transition. In fact, close to the transition, on the metallic side, as temperature decreases, the conductance of the insulating part decreases significantly, and its contribution to the total conductance is dramatically reduced. Since the critical percolation cluster is very ramified (in fact of fractal dimension), the contribution of the insulating part of the system dominates at high temperatures, and the increase of its resistance with decreasing temperature leads to an increase of the resistance as temperature is lowered, even on the metallic side. At low enough temperatures, however, when the resistance of the insulating part of the network becomes high enough, its contribution to the total conductance becomes negligible. Then the total resistance is dominated by the percolating conducting network, and thus the overall resistance will decrease with decreasing temperature. This leads to a nonmonotonic temperature dependence on the metallic side of the critical point, which can be clearly observed both in the model (Fig. 2c) and in the data (Fig. 2d).

The fact that only deep in the metallic regime, the overall resistance increases with increasing temperature, suggests that the density at which the resistance is approximately temperature independent is not the true critical point, but rather deeper on the metallic side. This is clearly seen in Fig. 3b, where one can see a point where all the low-temperature curves nearly cross, well inside the metallic regime. The above discussion suggests that one should be cautious in associating the critical point with the experimentally observed “temperature-independent” point (Fig. 3a), as done routinely in the experiment interpretations.

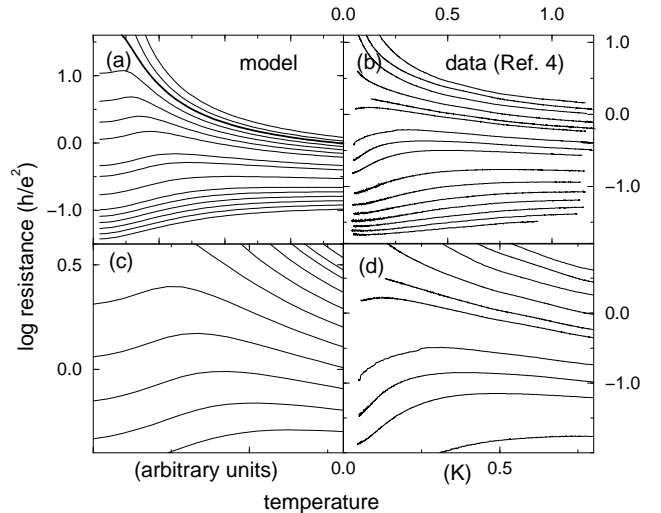


Fig. 2. Temperature dependence of the resistance for systems of different densities, as obtained by the model (a) and compared to the experimental data of Ref. [4] (b). The critical line is denoted by the bold curve. All curves below the critical line saturate at zero temperature, while above it the resistance diverges. For systems close to the transition on the metallic side, the resistance is a nonmonotonic function of temperature, as seen both in the model (c) and in the data (d).

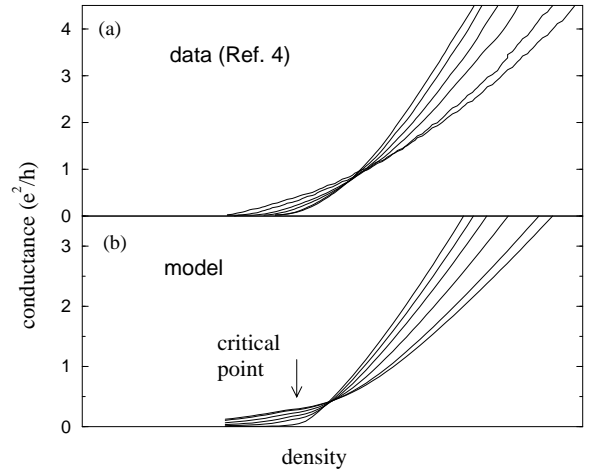


Fig. 3. Comparison of the density dependence of the conductance between the data of [4] (a) and the model (b), for several temperatures. The density at which the theoretical curves seem to cross each other, is well above the true critical point.

Lastly, The resistance at the metallic regime is given by some geometrical factor times the inverse of  $\sigma_m$  (Eq. 2), which naturally gives the observed exponential temperature dependence observed experimentally. The high-temperature resistance of the critical density network is

naturally around  $h/e^2$ , the only resistance scale in this model.

## V. PARALLEL MAGNETIC FIELDS

The effect of a parallel magnetic field on the overall conductance is determined by the way it affects the individual points contacts. The effect of a parallel field on transport through a single QPC has been studied in detail [24]. These experimental and theoretical studies demonstrated that the threshold density where the QPC opens up increases parabolically with the in-plane magnetic field. This effect was attributed to coupling of the in-plane motion to the strong confinement in the vertical direction, leading to an increase in the confining energy. Writing, for simplicity, the three dimensional Hamiltonian that describes free motion in two-dimensions and a harmonic confining potential in the third ( $z$ ) direction, with a magnetic field pointing in the  $x$ -direction

$$\mathcal{H} = \frac{p_x^2}{2m} + \frac{(p_y + eBz)^2}{2m} + \frac{p_z^2}{2m} + \frac{1}{2}m\omega_0^2 z^2 , \quad (5)$$

it is straightforward to see that the bottom of the 2d band shifts from  $\hbar\omega_0/2$  to  $\hbar\sqrt{\omega_0^2 + \omega_c^2}/2$ , with  $\omega_c \equiv eB/mc$ , leading to a corresponding decrease in the kinetic energy of all electrons. Thus the effective critical Fermi energy, or density, becomes larger. In other words, for a given density or chemical potential, if the system at zero field is on the metallic side, i.e. if the Fermi momentum is above the critical momentum (or kinetic energy) allowing percolation through the system, a parallel field will lower that energy towards the critical energy, eventually crossing the critical point and leading to an insulating behavior. Fig. 4 depicts the experimental data of [25], and the corresponding predictions of the model. As expected, as magnetic field increases, the system gradually crosses over from a metallic to an insulating behavior.

The above discussion allows a quantitative prediction of the effective critical energy in a parallel field ,

$$\epsilon_c(H) = \epsilon_c(H = 0) + \hbar \left( \sqrt{\omega_0^2 + \omega_c^2} - \omega_0 \right) / 2. \quad (6)$$

At zero temperature, when the resistance on the insulating side is infinite, we expect the resistance on the metallic side  $\mu > \epsilon_c(H = 0)$  to diverge with increasing field,

$$R(H) \sim (\mu - \epsilon_c(H))^{-t}. \quad (7)$$

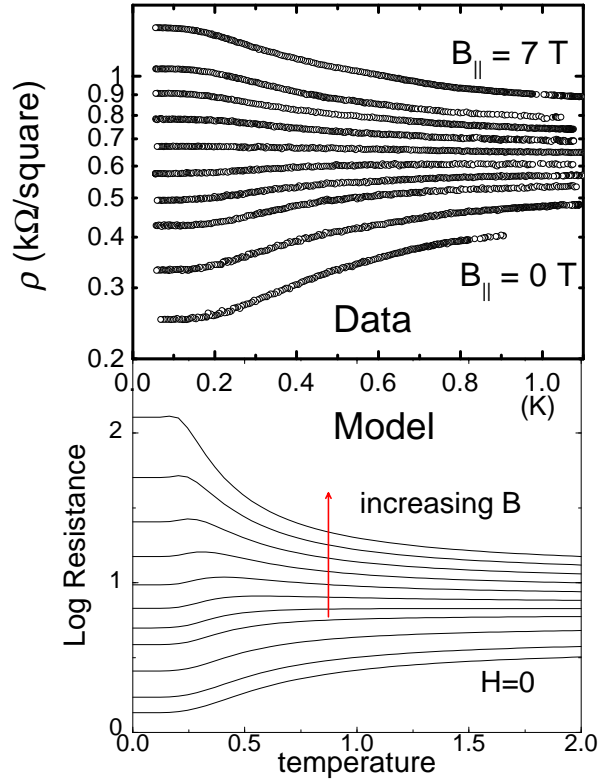


Fig. 4. Comparison between the experimental data [25] and the predictions of the model, demonstrating that a parallel magnetic field causes the metallic system to cross over gradually to the insulating regime.

For a finite temperature this divergence is cut off by the finite resistance of the insulator, and the magnetic field dependence changes as one crosses into the insulating side. This behavior is clearly seen in the experimental data of [25] (very similar data was also reported by Mertes et al. [26]). Fig. 5 depicts the experimental data [25] for the magnetic field dependence of the resistance, compared to what is expected from the model. The difference in behavior between the metallic and the insulating regimes is clear. On the metallic side we see that the resistance increases rapidly as the magnetic field brings the critical point closer to the chemical potential and then an abrupt change of behavior as the system enters the insulating regime. If the system was on the insulating side to begin with, then the magnetic field dependence of the resistance is similar to what is usually seen in systems where transport is via variable-range hopping [27]. In these system the positive magnetoresistance is due to spin polarization [28]. The magnetic field dependence on the insulating side depicted in Fig. V is assumed here to be due to that process. In this regime, however, the magnetic field at which there is a marked change in behavior is spin-related and should depend only weakly on density. A recent experimental investigation of the magnetoresistance in the insulating side [29] indeed supports this mechanism.

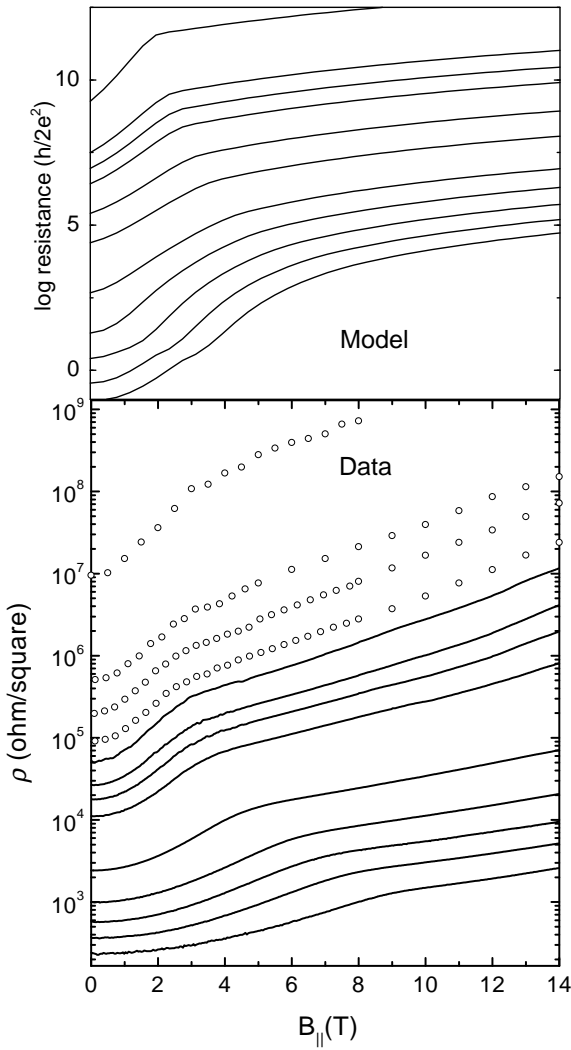


Fig. 5. Comparison of the experimentally measured resistance, as a function of parallel magnetic field [25] to the model predictions. On the metallic side, the magnetic field shift the critical point towards the chemical potential, leading to a divergence in the resistance, which is cut off by finite temperature.

As was mentioned above, the critical point in the density – magnetic field plane shifts towards higher densities with increasing magnetic field. Yoon et al. [25] have also measured the dependence of the critical field on density, which can be deduced from the inversion of Eq.(6),

$$H_c = m^*c/e\sqrt{\Delta(H)^2 + 2\hbar\omega_0\Delta(H)}, \quad (8)$$

where  $\Delta(H) \equiv \epsilon_c(H) - \epsilon_c(H = 0)$ . The comparison of the prediction of this simple equation to the data is depicted in Fig. 6 for two samples cut from the same wafer. The fitting parameters are the zero-field critical point,

that can be read directly from the data, the gate capacitance - the rate at which the Fermi energy changes with density, and the confining energy in the perpendicular direction,  $\hbar\omega_0$ . It is encouraging to note that while the critical energy, which is determined by the disorder realization, and the gate capacitance, which is determined by the geometry, are different for the two samples, both sets of data can be fitted by the same value of the perpendicular confining energy, which ought to be the same for the two samples, and turns out to be  $\hbar\omega_0 \simeq 0.8\text{meV}$ , leading to an extension of the wavefunction in the perpendicular direction of the order of 11 nm, similar to the value used by the authors of Ref. [15] to fit their experimental data.

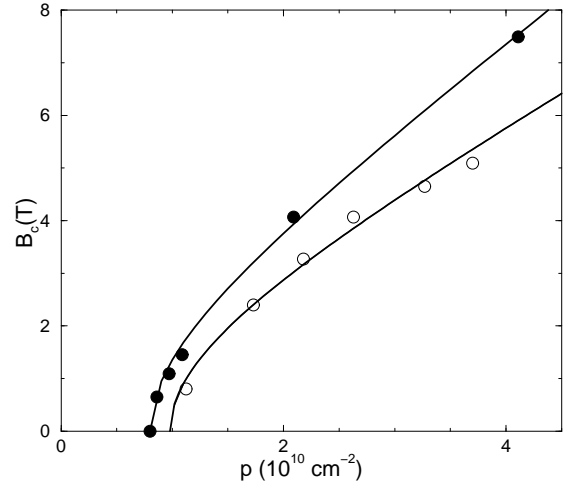


Fig. 6. Comparison of the measured density dependence of the critical magnetic field [25] (circles) to the prediction of the theory (Eq.8, solid lines). The two data sets are two different samples cut from the same wafer, and can be fitted using the same value of the perpendicular confining energy.

Interestingly, it seems that the effects of parallel fields can be understood without employing the electron spin. As a parallel field will also reduce the conductance of some of the point contacts from  $2e^2/h$  to  $e^2/h$ , the Zeeman effect will also increase the system's resistance. It should be noted that while the coupling of the in-plane motion to the confining potential in the perpendicular direction was also considered by Das Sarma and Hwang [30], the magnetoresistance predicted here, in contrast with Ref. [30], should not exhibit any anisotropy. The reason is that the direction of transport through the quantum point contacts is expected to be random, with no preferred direction.

## VI. PERPENDICULAR MAGNETIC FIELDS

While the longitudinal resistance depends exponentially on temperature, the weak field Hall resistance is

practically independent of temperature [31]. Such an observation might be hard to account for in theories that argue for new non-Fermi liquid-like behavior, but it is trivial in the present model - the critical exponent for the Hall coefficient in a two dimensional percolation problem is exactly zero [32], and thus the Hall coefficient should display no critical behavior at the critical point. This prediction was indeed confirmed in classical percolation experiments [33], and is very similar to that observed by Pudalov et al. [31].

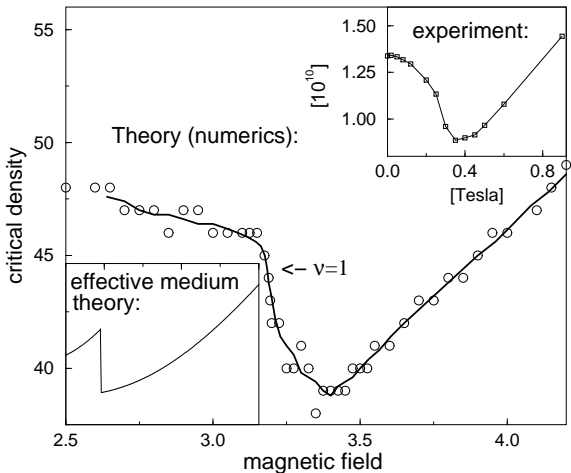


Fig. 7. The critical density - the number of electrons in the puddle, so that the topmost energy will allow transport through the point contact - as a function of magnetic field, in the presence of a finite disorder. The continuous curve is an averaged fit through the (necessarily integer) data points. Top-right inset: the corresponding experimental data [39]. Bottom-left inset: results of effective medium theory [36].

The situation in larger perpendicular magnetic fields is more interesting, as quantum Hall (QH) states are formed. Transport through a single QPC in perpendicular field and the crossover between the zero field limit and the QH limit have been studied in detail [34]. As expected, one finds that the critical energy oscillates with magnetic field due to the depopulation of Landau levels. In the present case, the oscillations are smoothed out by the disorder and by the averaging over many QPCs. Thus only the strongest oscillation, near  $\nu = 1$ , may survive, leading to a single dip in the critical density vs. magnetic field plot, as was observed experimentally. In order to allow for the averaging procedure, one has to take the full conductance distribution into account, which is beyond the two-species scaling theory. For completeness I report here results of numerical calculations [1] and effective medium theory [35,36]. In the numerical calculation I studied the energy levels of one puddle of electrons, which we modeled by a circular disk, in the presence of disorder [37]. In Fig. 7 I plot the “critical density” – the number

of electrons that need to occupy the puddle, so that the energy of the highest-energy electron will be enough to transverse the QPC [38], equivalent in the bulk system to the critical density – as a function of magnetic field. Indeed a dip near  $\nu = 1$  is clearly seen, with all other oscillations smoothed out by the disorder. This curve has a strong resemblance to the experimental data [39] (top-right inset). The results of the effective medium theory are depicted in the bottom-left inset, again demonstrating a dip near  $\nu = 1$ . In addition, it is expected that as the magnetic field is lowered below the  $\nu = 1$  minimum, more than one channel will transverse some QPCs, leading to an increase in the critical conductance, as indeed reported experimentally.

## VII. REDUCTION FACTORS LARGER THAN 2

In the degenerate electron limit ( $T \ll E_F$ ), the biggest reduction factor in the resistance on the metallic side, with decreasing temperature is a factor of 2. On the other hand, reduction factors close to an order of magnitude and even larger [40] have been observed experimentally, especially in Silicon based samples. Here I show that when temperature becomes of the same order of magnitude of  $E_F$ , the reduction factor in the model can assume arbitrarily large factors [41].

The electron density is given by

$$n = \int_0^\infty d\epsilon \frac{\rho_0}{1 + \exp[(\epsilon - \mu)/T]} = \rho_0 T \log [1 + \exp(\mu/T)] \quad (9)$$

where  $\rho_0$ , assumed constant, is the electronic density of states (per energy and per volume), and  $\mu$ , the chemical potential, is measured relative to the bottom of the band. Inverting the above equation, the chemical potential for a given density, is

$$\mu = T \log [\exp(n/\rho_0 T) - 1] \equiv T \log [\exp(E_F/T) - 1] \quad (10)$$

where the Fermi energy is defined as the  $T \rightarrow 0$  limit of the chemical potential. These textbook expressions demonstrate that while the Fermi energy varies linearly with the density, the chemical potential may be more sensitive to density variations in the nondegenerate limit  $T \sim E_F$ . Moreover, the chemical potential is now temperature dependent, and decreases with increasing temperature (see inset in Fig. 8). Substituting the above expression in the expression for the conductance through a single point contact (1) demonstrates that the conductance can decrease arbitrarily with increasing temperature (or, equivalently, that the resistance can decrease by an arbitrary factor with decreasing temperature). In Fig. 8 the temperature dependence of the conductance is plotted for two values of the Fermi energy,  $E_F$ . The curve for  $E_F \gg T$  shows the expected behavior for the degenerate electron gas - the conductance decreases and

saturates at a value smaller from the zero temperature conductance by a factor of 2. On the other hand, in the nondegenerate regime,  $E_F \sim T$ , the conductance decreases by a much larger factor.

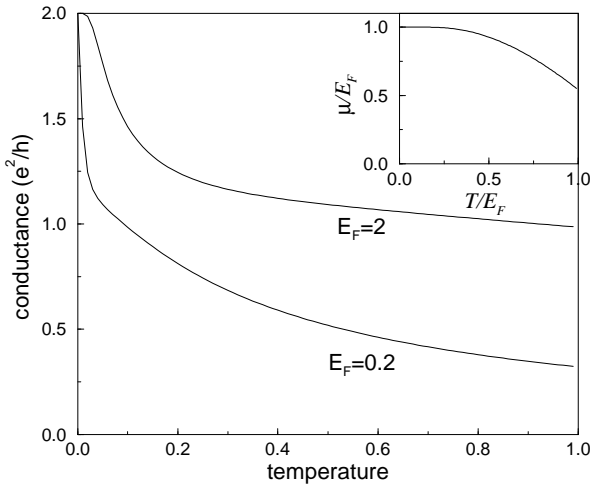


Fig. 8. The temperature dependence of the conductance in the degenerate ( $kT \ll E_F$ ) and in the degenerate regime ( $kT \simeq E_F$ ). While in the nondegenerate regime, the conductance can decrease by a factor of two, it can decrease arbitrarily in the nondegenerate regime, due to the temperature dependence of the chemical potential (inset).

### VIII. CONCLUSIONS

All the above results and discussion demonstrated that many of the experimental observations can be explained in the context of the simple semi-classical, noninteracting model introduced here. This is not to say that interactions and other effects are irrelevant. For example, the formation of the electron puddles may be dominated by interaction effects (see, e.g., Ref. [13]), and dephasing is certainly dominated, at these low temperatures, by electron-electron interactions. Other effects, including the energy dependence of the transmission coefficient and the possibility of more than one channel through the QPCs, the role of interband-scattering [6] and temperature-dependent impurities [8] may also be important to understand quantitative aspects of the data. Nevertheless, the fact that several important aspects of the experimental data can be explained in the context of a simple model is quite encouraging.

Some predictions made in [1], where the model was presented, were already confirmed. The mechanism for the quenching of the metallic phase by a parallel magnetic field was suggested there, and, as discussed above, agrees very well with recent experiments. Moreover, it was suggested that local measurements will be able to explore the percolative nature of the insulating phase.

Indeed, Ilani et al. [15] have used local probes to measure the change of the local chemical potential with density. While on the metallic side the signals from all probes were identical, and were accurately described by Hartree-Fock theory, these probes gave different signals on the insulating side, which the authors interpreted as a signature of a percolative phase. (An indirect experimental verification of the percolation process in the QH regime was already reported in [42]). As the metallic puddles can be thought of as quantum dots, one can use the abundant information about such structures [43], to gain additional understanding of the characteristics of the puddles and the phase separation. Such local probes [44] can give a "smoking gun" verification of the picture presented here by looking for the periodic oscillations of the local chemical potential on the insulating side, due to depopulation of the Landau levels, as was observed in quantum dots [46].

To conclude, a semi-classical model, combining local quantum transport and global classical percolation was employed to explain the observed metal-insulator transition. The model attributes the transition to the finite dephasing length in these temperatures. As temperature is lowered even further, and the dephasing length becomes larger than the puddle size, quantum localization effects should kick in. Such weak-localization corrections in the metallic side were indeed observed experimentally, confirming the expectation that, if the dephasing length indeed diverges at zero temperature, these systems will eventually become Anderson insulators.

I thank many of my colleagues for fruitful discussions: A. Auerbach, Y. Gefen, Y. Hanein, P. McEuen, D. Shahar, E. Shimshoni, U. Sivan, A. Stern, N. S. Wingreen, A. Yacoby and Y. Yaish. In particular, I would like to thank Y. Hanein & D. Shahar and U. Sivan & Y. Yaish for making their data available to me. This work was supported by THE ISRAEL SCIENCE FOUNDATION - Centers of Excellence Program, and by the German Ministry of Science.

---

[1] Y. Meir, *Phys. Rev. Lett.*, **83**, 3506 (1999).  
[2] S. V. Kravchenko et al., *Phys. Rev.* **B50**, 8039 (1994); *ibid.*, **51**, 7038 (1995); *Phys. Rev. Lett.* **77**, 4938 (1996); V. M. Pudalov et al., *JETP Lett.* **65**, 932 (1997); D. Popović et al., *Phys. Rev. Lett.* **79**, 1543 (1997); K. Ismail et al., cond-mat/9707061; J. Lam et al., *Phys. Rev.* **B56** R12741 (1997).  
[3] P. T. Coleridge et al., *Phys. Rev.* **B56**, R12764 (1997); M. Y. Simmons et al., *Phys. Rev. Lett.* **80**, 1292 (1998).  
[4] Y. Hanein et al., *Phys. Rev. Lett.* **80**, 1288 (1998); *Phys. Rev.* **B58**, R7520 (1998).  
[5] Y. Hanein et al., *Phys. Rev.* **B58**, R13338 (1998).  
[6] Y. Yaish and el., cond-mat/9904324, and unpublished.

[7] E. Abrahams et al., *Phys. Rev. Lett.* **42**, 673 (1979).

[8] B. L. Altshuler and D. L. Maslov, *Phys. Rev. Lett.* **82**, 145 (1999). B. L. Altshuler, D. L. Maslov, V. M. Pudalov, cond-mat/9909353. See also, S. V. Kravchenko, M. P. Sarachik, and D. Simonian, *Phys. Rev. Lett.* **83**, 2091 (1999); B. L. Altshuler and D. L. Maslov, *ibid* 2092 (1999).

[9] G. Benenti, X. Waintal and J.-L. Pichard, *Phys. Rev. Lett.* **83**, 1826 (1999).

[10] A. M. Finkelstein, *Zh. Eksp. Teor. Fiz.* **84**, 168 (1983); *Z. Phys.* **56**, 189 (1984); C. Castellani et al., *Phys. Rev.* **30**, 527 (184; *ibid* 1596 (1984).

[11] V. Dobroslavljević et al., *Phys. Rev. Lett.* **79**, 455 (1997); C. Castellani, C. Di Castro, and P. A. Lee, *Phys. Rev.* **B57**, R9381 (1998); D. Belitz and T. R. Kirkpatrick, *Phys. Rev.* **B58**, 8214 (1998); P. Phillips et al., *Nature (London)* **395**, 253 (1998); F.-C. Zhang and T. M. Rice, cond-mat/9708050; S. Chakravarty, et al., *Phil. Mag. B* **79**, 859 (1999).

[12] V. M. Pudalov, *JETP Lett.* **66**, 175 (1997).

[13] Song He and X. C. Xie, *Phys. Rev. Lett.* **80**, 3324 (1998). J. Shi, Song He and X.C. Xie, *Physical Review B* **60**, R13950 (1999).

[14] E. Ribeiro et al., *Phys. Rev. Lett.* **82**, 996 (1999).

[15] S. Ilani et al., cond-mat/9910116.

[16] M. Y. Simmons et al., cond-mat/9910368; G. Brunthaler et al., cond-mat/9911011.

[17] V. Senz et al., cond-mat/9910228;

[18] G. Eytan et al., *Phys. Rev. Lett.* **81**, 1666 (1998).

[19] D. P. Pivin et al., *Phys. Rev. Lett.* **82**, 4687 (1999); A. G. Huibers et al., cond-mat/9904274.

[20] E. Shimshoni and A. Auerbach, *Phys. Rev. B* **55**, 9817 (1997); E. Shimshoni, A. Auerbach and A. Kapitulnik, *Phys. Rev. Lett.* **80**, 3352 (1998).

[21] At lower temperatures variable-range hopping [See, e.g., B. I. Shklovskii and A. L. Efros, *Electronic Properties of Doped Semiconductors* (Springer-Verlag, Berlin, 1984)] will become relevant, but is ignored here, again to avoid additional parameters, except in Sec. V.

[22] A. L. Efros and B. I. Shklovskii, *Phys. Stat. Sol.* **B76**, 475 (1976); A. Bunde et al., *J. Phys. A* **18**, L137 (1985).

[23] For a review of percolation theory and for values of the critical exponents, see, for example, D. Stauffer and A. Aharaony, *Introduction to Percolation Theory* (Taylor & Francis, London, 1992).

[24] T. P. Smith et al., *Phys. Rev. Lett.* **61**, 585 (1988); K. J. Thomas et al., *Phys. Rev. Lett.* **77**, 135 (1996); *Phys. Rev.* **B58**, 4846 (1998).

[25] J. Yoon et al., cond-mat/9907128.

[26] M. Mertes et al., *Phys. Rev. B* **50**, R5093 (1999).

[27] See, e.g., A. Vaknin et al., *Phys. Rev. B* **54**, 13604 (1996).

[28] A. Kurobe and H. Kamimura, *J. Phys. Soc. Jpn* **51**, 1904 (1982); H. Kamimura, *Prog. Theor. Phys.* **72**, 206 (1982); See also Y. Meir, *Europhys. Lett.* **33**, 471 (1996).

[29] V. I. Kozub et al., cond-mat/9911450.

[30] S. Das Sarma and H. Hwang, cond-mat/9909452.

[31] V. M. Pudalov et al., *JETP lett.* **70**, 48 (1999).

[32] B. I. Shklovskii, *Sov. Phys. JETP* **45**, 152 (1977); J. P. Straley, *J. Phys. C* **10**, 3009 (1977).

[33] See, e.g., A. Palevski et al., *J. Phys. Lett. (Paris)* **45**, L367 (1984).

[34] See, e.g., B. J. van Wees, *Phys. Rev. B* **43**, 12431 (1991).

[35] S. Kirkpatrick, *Phys. Rev. Lett.* **25**, 807 (1970);

[36] Y. Meir, to be published.

[37] To simplify the numerics, I chose random potentials with azimuthal symmetry.

[38] H. A. Fertig and B. I. Haleprin, *Phys. Rev. B* **36**, 7969 (1987).

[39] Y. Hanein et al., *Nature* **400**, 735 (1999).

[40] V. M. Pudalov et al., *Phys. Rev. B* **60**, R1254 (1999).

[41] P. McEuen, private communication.

[42] A. A. Shashkin et al., *Phys. Rev. Lett.* **73**, 3141 (1994); V. T. Dolgopolov et al., *JETP Lett.* **62**, 162 (1995); I. V. Kukuskin et al., *Phys. Rev. B* **53**, R13260 (1996).

[43] For recent reviews on quantum dots see, e.g., M. A. Kastner, *Comm. Cond. Matt.* **17**, 349 (1996); R. Ashoori, *Nature* **379**, 413 (1996).

[44] See, e.g., S. H. Tessmer et al., *Nature* **392**, 6671 (1998); H. F. Hess et al., *Solid Stat. Comm.* **107**, 657 (1998).

[45] C. Pasquier et al., *Phys. Rev. Lett.* **70**, 69 (1993).

[46] P. L. McEuen et al., *Phys. Rev. Lett.* **66**, 1926 (1991).